HHS Public Access

Author manuscript

Nat Med. Author manuscript; available in PMC 2012 June 21.

Published in final edited form as:

Nat Med. 2011 May ; 17(5): 618–622. doi:10.1038/nm.2332.

Brain PPARγ Promotes Obesity and is Required for the Insulin–Sensitizing Effect of Thiazolidinediones

Min Lu[1], **David A. Sarruf**[2], **Saswata Talukdar**[1], **Shweta Sharma**[1,3], **Pingping Li**[1], **Gautam Bandyopadhyay**[1], **Sarah Nalbandian**[1], **WuQiang Fan**[1], **Jiaur R. Gayen**[1,3], **Sushil K. Mahata**[1,3], **Nicholas J. Webster**[1,3], **Michael W. Schwartz**[2,4], and **Jerrold M. Olefsky**[1,4]

[1] Department of Medicine, University of California, San Diego, CA 92093

[2] Diabetes and Obesity Center of Excellence, University of Washington, Seattle, WA 98104

[3] Medical Research Service, Veterans Affairs San Diego Healthcare System, San Diego, CA92093

Abstract

In adipose, muscle, liver and macrophages, signaling by the nuclear receptor PPARγ is a determinant of insulin sensitivity and this receptor mediates the insulin–sensitizing effects of thioazolidinediones (TZDs)[1-4]. Since PPARγ is also expressed in neurons[5], we generated mice with neuron–specific *Pparγ* knockout (*Pparγ* BKO) to determine whether neuronal PPARγ signaling contributes to either weight gain or insulin resistance. During high fat diet (HFD) feeding, food intake was reduced and energy expenditure increased in *Pparγ* BKO mice, resulting in reduced weight gain. When treated with the TZD rosiglitazone, *Pparγ* BKO mice were resistant to rosiglitazone–induced hyperphagia and weight gain and, relative to rosiglitazone–treated controls, experienced only a marginal improvement in glucose metabolism. Hyperinsulinemic euglycemic clamp studies showed that the effect of rosiglitazone treatment to increase hepatic insulin sensitivity during HFD feeding was completely abolished in *Pparγ* BKO mice, an effect associated with the failure of rosiglitazone to improve liver insulin receptor signal transduction. We conclude that excess weight gain induced by HFD feeding depends in part on the effect of neuronal PPARγ signaling to limit thermogenesis and increase food intake. Neuronal PPARγ signaling is also required for the hepatic insulin sensitizing effects of TZDs.

[4] Co–corresponding authors Address correspondence to Jerrold M. Olefsky jolefsky@ucsd.edu or Michael W. Schwartz mschwart@u.washington.edu.

DISCLOSURE STATEMENT: The authors have nothing to disclose.

Contributions

J.M.O., M.L., and M.W.S designed the study and co-wrote the manuscript. M.L. performed most of the experiments. D.A.S was responsible for body composition, locomotor activity, indirect calorimetry, and leptin sensitivity assay. S.T. conducted most of the qPCR and performed acute insulin stimulation in mice. S.S and N.J.W. were involved in mouse breeding and performed IHC. P.L was involved in hyperinsulinemic euglycemic clamp and Western blotting. G.B measured tissue lipid content. S.N was involved in metabolic studies in mice. W.F contributed to Western blotting. J.R.G and S.K.M are responsible for measurement of cardiac function and catecholamine concentratoins.

Keywords

PPARγ; Central Nervous System; rosiglitazone; Insulin Sensitivity; Hyperphagia

Thiazolidinediones (TZDs) are a class of drugs that activate peroxisome proliferator–activated receptor γ (PPARγ) and improve blood glucose control and systemic insulin sensitivity in patients with type 2 diabetes mellitus (T2DM)[6]. In addition to enhancing insulin action, TZDs induce weight gain in humans and rodent models not only via enhanced adipogenesis and fluid retention, but by increasing food intake[7,8]. This latter effect suggests that PPARγ signaling in the central nervous system (CNS) may influence energy intake and storage. Consistent with this hypothesis, PPARγ is expressed in key brain areas involved in energy homeostasis and glucose metabolism[5], raising the possibility that the CNS might be a previously unrecognized site for TZD action.

To investigate the function of neuronal PPARγ, we generated brain–specific *Pparγ* knockout mice (*Pparγ* BKO mice) using the synapsin I Cre–LoxP system. Cre expression driven by the Synapsin I promoter (Syn–Cre mice) leads to recombination in neurons, but not other cell types[9]. To verify brain–specific deletion of *Pparγ* in BKO mice, we isolated RNA from multiple brain regions and from peripheral tissues for measurement of *Pparγ* mRNA abundance. Quantitative PCR (qPCR) showed that brain *Pparγ* deletion was regional, with markedly reduced mRNA abundance in spinal cord, brain stem, hypothalamus, diencephalon and hippocampus, mildly reduced expression in cerebral cortex, and unchanged levels in cerebellum and olfactory bulb, compared to control mice (**Fig. 1a**). We further confirmed neuron–specific deletion in the *Pparγ* BKO mice by double–staining for PPARγ and the neuronal marker NeuN, and found that PPARγ is expressed in both neurons and non–neuronal cells in the CNS, albeit with distinctive patterns in different regions. In hippocampus, for example, most $PPAR\gamma^+$ cells were also $NeuN^+$ and, accordingly, the number of double positive cells was reduced in BKO mice (**Supplementary Fig. 1**). In contrast, the majority of $PPAR\gamma^+$ cells in the cortex were $NeuN^-$, indicating non–neuronal PPARγ expression. These histochemical data are fully consistent with the qPCR analysis, showing a much greater reduction of *Pparγ* mRNA in hippocampus than in cortex of BKO mice.

PCR detection of genomic DNA (data not shown) and RNA (**Fig. 1b**) from various tissues demonstrated Cre–mediated recombination in brain, but not in muscle, liver, adipose tissue, pancreas or other tissues. We also confirmed that tissues other than brain displayed normal *Pparγ* expression (**Fig. 1c**).

Body weights of *Pparγ* BKO mice fed a standard chow diet were slightly, but significantly, lower than control mice at a young age (8–11wk), but these differences were transient, disappearing by age 13 wk (**Supplementary Fig. 2a**). Metabolic studies on chow fed mice did not reveal any difference between genotypes (**Supplemental Fig. 2b–f**).

When 12–wk old control and *Pparγ* BKO mice were placed on a HFD, the body weight curves diverged over a 7–wk period, with reduced weight gain in BKO mice (**Fig. 2a**). Body composition analysis revealed that this weight difference was due to a reduced body fat

percentage in BKO mice compared to controls fed the same HFD (**Fig. 2b**). To determine whether differences in energy intake, energy expenditure, or both contribute to the lean phenotype of BKO mice, we measured food intake and metabolic parameters during HFD feeding. Ambulatory activity and oxygen consumption were increased in BKO mice, compared to controls, in both dark and light cycles (**Fig. 2c**). Multiple regression analysis[10] demonstrated increased energy expenditure in BKO mice after adjusting for differences of body weight, composition, and physical activity (**Fig. 2d and Supplementary Table 1**). Since BKO mice also consumed less food over the course of 12 wk of HFD feeding (**Fig. 2e**) than controls, their protection against HFD–induced obesity involves both increased energy expenditure and reduced energy intake, indicating that neuronal PPARγ signaling is required for the effects of HFD feeding on both sides of the energy balance equation.

Leptin is an adipokine that increases energy expenditure and reduces energy consumption via central effects[11] and the effects of HFD feeding to reduce leptin sensitivity are well established. Since *Pparγ* BKO mice are protected against excess weight gain on this diet, we hypothesized that neuronal PPARγ signaling contributes to leptin resistance in this setting. Although the basal circulating leptin concentration was comparable in both genotypes (**Fig. 2f**), leptin sensitivity was increased in BKO mice when measured as the effect on food intake of leptin administration for 48 h. Leptin induced a larger decrease of food intake in BKO mice fed standard chow compared to either f/f mice or Syn–Cre mice (**Supplementary Fig. 3a**), despite no differences in body weight among these three groups (data not shown). A similar, but statistically insignificant ($p = 0.14$), trend was observed in HFD–fed BKO mice (**Supplementary Fig. 3b**). Thus, neuronal *Pparγ* deficiency appears to sensitize mice to leptin's anorexigenic effects. To assess leptin responsiveness using a biochemical approach, we measured phosphorylation of STAT3, a downstream mediator of intracellular lepin signaling, in hypothalamic extracts following a single intraperitoneal leptin injection. As expected, HFD feeding caused leptin resistance in control mice, as indicated by the failure of leptin to increase hypothalamic phospho–STAT3 (Y705) levels[12]. In contrast, hypothalamic phospho–STAT3 levels were increased in leptin–relative to vehicle–treated BKO mice (**Fig. 2g**). Although these studies are clearly indicative of a leptin signaling defect in the brain, additional experiments will be essential to further define the abnormalities in this signaling pathway and their pathophysiologic effects. In this latter experiment, the basic phenotype of the BKO mice is that they weigh less than controls so their increased biochemical leptin sensitivity could have been secondary to their protection against obesity rather than a direct consequence of neuronal *Pparγ* deficiency. Although future studies are warranted to address this issue, in either case these data collectively indicate that the phenotype of BKO mice includes increased leptin sensitivity.

To determine whether neuronal PPARγ signaling contribute to the actions of TZD's, we fed mice a HFD to induce obesity and insulin resistance, followed by HFD supplemented with rosiglitazone. As expected, the addition of rosiglitazone led to an increase of body weight and food intake in both f/f mice and Syn–Cre mice compared to age–matched mice fed the same diet without rosiglitazone for the same period of time (28–34 weeks of age) (**Fig. 3a–c**). Relative to control mice, the effects of rosiglitazone to increase food intake and body weight in *Pparγ* BKO mice were attenuated by ~50% (delta body weight in f/f *vs.* BKO

mice = 4.7 *vs.* 2.2 gm; **Fig. 3a–c**). To further characterize this aspect of the BKO phenotype, we initiated HFD and rosiglitazone treatment simultaneously in chow–fed mice. As expected, the resulting weight gain over the subsequent 2–wk period was substantially less in BKO mice than in controls (**Supplementary Fig. 3c**). Thus, neuronal PPARγ is required, at least in part, for TZD–induced hyperphagia and weight gain.

The increased energy expenditure observed in *Pparγ* BKO mice prompted us to assess the expression of thermogenic genes in brown and white adipose tissue. Consistent with previous publications[13], rosiglitazone administration to control mice increased expression of *Ucp1* mRNA in white adipose tissue (WAT) and *Ucp3* mRNA in liver and muscle (**Fig. 3d–h**). Notably, *Ucp1* mRNA expression in WAT of BKO mice were higher than control values before rosiglitazone treatment, and TZD treatment enhanced WAT *Ucp1* mRNA expression in BKO mice to a greater extent than in controls (**Fig. 3d**). Thus, the effect of TZD to increase WAT *Ucp1* expression is enhanced in mice with neuron–specific *Pparγ* deletion. *Ucp1* mRNA content in BAT was also elevated in BKO mice (**Fig. 3e**), and this effect was associated with decreased BAT lipid accumulation (**Fig. 3f**). In muscle, *Ucp3* mRNA expression was similar between genotypes both before and after rosiglitazone treatment (**Fig. 3g**) whereas in liver, rosiglitazone induction of *Ucp3* expression was markedly augmented in BKO mice (**Fig. 3h**). These observations collectively identify mitochondrial uncoupling in WAT and other tissues as a likely mechanism to explain increased energy expenditure in mice with neuronal *Pparγ* deficiency. By extension, we infer a physiological role for neuronal PPARγ signaling to limit expression of UCP proteins in adipose tissue and liver and thereby limit energy expenditure.

Since increased mitochondrial uncoupling in adipose tissue can result from increased thyroid hormone signaling, we assessed the thyroid axis in *Pparγ* BKO mice. We found that these animals exhibit normal plasma thyroid hormone concentrations (**Supplementary Figs. 3d and e**) and normal hypothalamic expression of both the thyroid hormone receptor and thyrotropin releasing hormone (**Supplementary Fig. 3f**). Thus, altered thyroid function is an unlikely contributor to the hypermetabolic phenotype of these mice. Similarly, measures of blood pressure, heart rate, and catecholamine concentrations were the same between genotypes (**Supplementary Figs. 4a–c**) indicating that stress is not the mechanism driving the hypermetabolic phenotype of BKO mice.

We next evaluated the contribution of neuronal PPARγ to the control of insulin sensitivity in both the presence and absence of rosiglitazone. After either 3 or 7 wk of TZD treatment, glucose tolerance was markedly improved in HFD–fed control mice, but not in *Pparγ* BKO mice, despite equally reduced fasting free fatty acid (FFA) concentrations (**Fig. 4a and Supplementary Figs. 4d and e**). Hyperinsulinemic–euglycemic clamp measurements provide a quantitative assessment of insulin sensitivity *in vivo* and, as expected, we found that in control mice, rosiglitazone treatment significantly increased both the glucose infusion rate (GIR, a measure of whole–body insulin action) and the insulin–stimulated glucose disposal rate (IS–GDR) (**Fig. 4b and 4c**). At the same time, drug treatment lowered basal hepatic glucose production (HGP), while enhancing the ability of insulin to inhibit HGP (**Fig. 4d and 4e**).

Compared to control mice, *Pparγ* BKO mice were less insulin–sensitive after rosiglitazone treatment. Most strikingly, the beneficial effects of rosiglitazone on both basal HGP and insulin–induced suppression of HGP were completely abolished in the BKO mice (**Fig. 4d–f**), despite the fact that these mice consumed less food and gained less weight (**Fig. 3b and c**). Although GIR and IS–GDR values were moderately reduced in TZD–treated BKO mice, the incremental values for IS–GDR between the untreated and treated state were comparable (13 *vs.* 11 mg kg^{-1} min^{-1}) between genotypes.

In concert with the clamp studies, biochemical measures of hepatic insulin signaling were also blunted in TZD–treated *Pparγ* BKO mice relative to controls, as reflected by decreased AKT and GSK3 phosphorylation after acute insulin stimulation (**Fig. 4g and h**). Rosiglitazone–treated BKO mice also exhibited increased hepatic CREB phosphorylation and elevated PEPCK expression (**Fig. 4g and i**), whereas *Socs3* mRNA content was increased in rosiglitazone–treated BKO mice compared to controls (**Supplementary Fig. 5a**). Since SOCS3 is a negative regulator of insulin signaling, this latter effect could potentially contribute to liver insulin resistance in these mice during TZD treatment. Finally, liver DAG and ceramide concentrations were lowered by rosiglitazone treatment in both genotypes (**Supplementary Table 2**).

As shown in **Supplementary Figs 5b–d**, tissue inflammatory gene expression did not differ between genotypes, nor were circulating cytokine or adiponectin concentrations different between BKO mice and controls (**Supplementary Fig 6**). Thus, neither increased systemic inflammation nor differences in adiponectin levels can explain the relative insulin resistance of rosiglitazone–treated BKO mice.

Our results show surprising effects of brain PPARγ on food intake, energy expenditure, and insulin sensitivity. Deletion of brain *Pparγ* led to both reduced food intake and increased energy expenditure, effects that were specific to consumption of a HFD and which protected mice from excess weight gain and adiposity in this setting. One potential mechanism to explain this outcome is increased leptin sensitivity and associated increases of *Ucp1* expression in BAT and WAT, and *Ucp3* expression in liver of *Pparγ* BKO mice. Protection against rosiglitazone–induced hyperphagia and weight gain was also observed in BKO mice. Despite their reduced adiposity, these animals displayed impaired glucose tolerance and reduced insulin sensitivity during rosiglitazone treatment, compared to controls. Of particular relevance is the liver–specific nature of the impaired response to rosiglitazone in these mice, which implies that the effect of TZDs to improve insulin sensitivity in liver, but not in other tissues, involves a CNS mechanism. We conclude that neuronal PPARγ contributes to excess weight gain during HFD feeding and in response to TZD treatment, and is also required for the TZD–mediated improvement of liver insulin sensitivity. These studies define a new role for brain PPARγ as both an integrator of signals affecting energy balance and glucose homeostasis and as a target for the action of TZDs.

Online Methods

Animals

We backcrossed mice carrying *Pparγ* floxed alleles (f/f mice)[1] onto C57BL/6 background for >10 generations. We backcrossed transgenic mice harboring Cre recombinase under the control of the neuron–specific rat synapsin I promoter (Syn–Cre mice)[9] onto the C57BL/6 background for >6 generations. We bred f/f mice with Syn–Cre mice to generate *Pparγ* f/+ mice with a positive Cre gene, which were further bred with *Pparγ* f/f mice to obtain *Pparγ* BKO mice. Since occasional male mice carrying synapsin I Cre can generate germline deletion of the target gene in progeny due to expression of Cre recombinase in sperms[14], we screened all *Pparγ* BKO mice for germline deletion (e.g., heterozygous whole-body *Pparγ* KO mice), and such mice were eliminated from our studies. We housed mice in a 12 h light/12 h dark cycle. At 12–wk of age, mice were either fed normal chow diet (LabDiet, Cucamonga, CA) or 60% HFD (Research Diets, New Brunswick, NJ). At wk 16 on HFD, a subset of mice was switched to 60% HFD with rosiglitazone (3 mg kg^{-1} d^{-1}) for up to 10 wk.

Mouse procedures conformed to the Guide for Care and Use of Laboratory Animals of the US National Institutes of Health, and were approved by the Animal Subjects Committee of the University of California, San Diego.

Metabolic Studies

We performed hyperinsulinemic euglycemic clamp studies as previously described[15]. We only used mice that lost < 6% of their pre–cannulation weight after 4–5 days of recovery. The clamp experiments began with a constant infusion (5 μCi h^{-1}) of D–[3–3H] glucose (Du Pont–NEN, Boston, MA) in 6–h fasted mice. After 90 min of tracer equilibration and basal sampling, we infused glucose (50% dextrose; Abbott) and tracer (5 μCi h^{-1}) plus insulin (6 mU kg^{-1} min^{-1}) into the jugular vein. We drew small blood samples from the tail vein at 10–min intervals and confirmed the achievement of steady–state conditions (120 mg dl^{-1} ± 5 mg dl^{-1}) at the end of the clamp by maintaining glucose infusion and plasma glucose concentration for a minimum of 20 min. We took blood samples at t = –10, 0 (basal), 110, and 120 (end of experiment) min to determine glucose–specific activity and insulin concentration. We quantified tracer–determined rates by using the Steele equation for steady–state conditions[16]. At steady state, the rate of glucose disappearance, or total GDR, is equal to the sum of the rate of endogenous glucose productions (HGP) plus the exogenous (cold) GIR. The IS–GDR is equal to the total GDR minus the basal glucose turnover rate.

We performed other metabolic measurements as previously described[15,17,18]. For assay of biochemical responses to insulin stimulation, we anesthetized mice after a 6–h fast. We ligated vessels supplying one side of leg muscles, one lobe of the liver and one epididymal fat pad and took basal samples of liver, muscle, and fat. Five minutes after a bolus injection of insulin (1 U kg^{-1} via inferior vena cava), we harvested the remaining liver, muscle, and fat and snap froze to measure signal transduction markers.

Body Composition, Locomotor Activity, and Indirect Calorimetry

We measured mouse lean and fat mass using quantitative magnetic resonance spectroscopy (Echo Medical Systems, Houston, TX) after 5 wk of HFD. At wk 6 of HFD, we individually placed mice into metabolic cages for measurements. We adapted all animals to the novel environment for 48 h before study. We normalized VO2 and VCO2 using a multiple regression–based approach[10] to account for variation of both lean and fat mass. We calculated energy expenditure (EE) based on EE = 3.815 × VO2 + 1.232 × VCO2.

Biochemical Leptin Sensitivity Assays

After 8 weeks of HFD feeding, we injected overnight fasted f/f and BKO mice intraperitoneally with either vehicle or recombinant mouse leptin 1 mg kg^{-1} (National Institute of Diabetes and Digestive and Kidney Diseases and The National Hormone and Pituitary Program, Torrance, CA) and decapitated mice 90 min later. We rapidly dissected and froze the hypothalami for detection of phospho–STAT3 (Y705) and STAT3 by immunoblotting.

Western Blotting

We performed Western blotting as previously described[19]. We purchased all primary antibodies, except antibody to β–tubulin (Millipore, Billerica, MA), from Cell Signaling Technology, Inc. (Beverly, MA). We analyzed the protein bands using Image J densitometry analysis and normalized phosphorylated protein to total protein bands.

Gene Expression Analyses

We carried out quantitative PCR as previously described[15]. We measured mRNA of *Pparγ* using the following primer set: 5'–GTCACGTTCTGACAGGACTGTGTGAC–3' and 5'–GGGTCAGCTCTTGTGAATGGAATG–3', in which the reverse primer detects the exon absent in the mutant mice. We normalized the mRNA content of all genes reported to housekeeping genes (*cyclophilin A* and *RNA polymerase II*). For detection of mutant *Pparγ* mRNA, we used the following primer set that binds to sequence flanking the absent exons: 5'–GTCACGTTCTGACAGGACTGTGTGAC–3' and 5'–TATCACTGGAGATCTCCGCCAACAGC–3'.

Statistical Analysis

For experiments involving two factors, we analyzed data by two–way ANOVA followed by Bonferroni post tests using Prizm (GraphPad Software, Inc., San Diego, CA). We performed individual pair-wise comparisons using student t test in Excel (Microsoft, Redmond, WA).

Supplementary Material

Refer to Web version on PubMed Central for supplementary material.

Acknowledgements

We thank Pamela Mellon lab at UCSD for providing Syn–Cre mice. We thank J. Pimentel, A. Amidi, B. Scott, J. Meadows, and J. Ficsher for technical support. We thank D. Oh, J. Xu, E. Bae, O. Osborne, A. Chen, and D. Sears for helpful discussions. We thank the Histology and Immunohistochemistry Resource (L. Gapuz and N. Varki) at

the Rebecca & John Moores UCSD Cancer Center. This work was supported by US National Institutes of Health (NIH) grants DK033651, DK063491, DK074868 and DK09062 (to J. Olefsky) and by the Eunice Kennedy Shriver National Institutes of Child Health and Human Development/NIH through cooperative agreement of U54 HD012303–25 as part of the specialized Cooperative Centers Program in Reproduction and Infertility Research. This work was also supported by NIH Grants DK068384, DK083042 and DK052989 (to M. Schwartz), by Ruth L. Kirschstein National Research Service Award fellowship F32DK080604–01 (to D. Sarruf), and by the Nutrition Obesity Research Center grant DK035816 and the Mouse Metabolic Phenotyping Center (U24 DK076126) at the University of Washington. UCSD Cancer Center microscopy core is supported by the UCSD Cancer Center Specialized Support Grant P30 CA23100. Body composition and energy expenditure analyses were performed with support from the NIH-funded Mouse Metabolic Phenotyping Center at the University of Washington. Calorimetry was performed by K. Ogimoto and expert assistance in analyses of these data was provided by K. Kaiyala.

References

1. He W, et al. Adipose-specific peroxisome proliferator-activated receptor gamma knockout causes insulin resistance in fat and liver but not in muscle. Proceedings of the National Academy of Sciences of the United States of America. 2003; 100:15712–15717. [PubMed: 14660788]
2. Hevener AL, et al. Muscle-specific Pparg deletion causes insulin resistance. Nature medicine. 2003; 9:1491–1497.
3. Hevener AL, et al. Macrophage PPAR gamma is required for normal skeletal muscle and hepatic insulin sensitivity and full antidiabetic effects of thiazolidinediones. The Journal of clinical investigation. 2007; 117:1658–1669. [PubMed: 17525798]
4. Odegaard JI, et al. Macrophage-specific PPARgamma controls alternative activation and improves insulin resistance. Nature. 2007; 447:1116–1120. [PubMed: 17515919]
5. Sarruf DA, et al. Expression of peroxisome proliferator-activated receptor-gamma in key neuronal subsets regulating glucose metabolism and energy homeostasis. Endocrinology. 2009; 150:707–712. [PubMed: 18845632]
6. Semple RK, Chatterjee VK, O'Rahilly S. PPAR gamma and human metabolic disease. The Journal of clinical investigation. 2006; 116:581–589. [PubMed: 16511590]
7. Lehrke M, Lazar MA. The many faces of PPARgamma. Cell. 2005; 123:993–999. [PubMed: 16360030]
8. Shimizu H, et al. Troglitazone reduces plasma leptin concentration but increases hunger in NIDDM patients. Diabetes care. 1998; 21:1470–1474. [PubMed: 9727893]
9. Zhu Y, et al. Ablation of NF1 function in neurons induces abnormal development of cerebral cortex and reactive gliosis in the brain. Genes & development. 2001; 15:859–876. [PubMed: 11297510]
10. Kaiyala KJ, et al. Identification of Body Fat Mass as a Major Determinant of Metabolic Rate in Mice. Diabetes.
11. Morton GJ, Cummings DE, Baskin DG, Barsh GS, Schwartz MW. Central nervous system control of food intake and body weight. Nature. 2006; 443:289–295. [PubMed: 16988703]
12. Munzberg H, Flier JS, Bjorbaek C. Region-specific leptin resistance within the hypothalamus of diet-induced obese mice. Endocrinology. 2004; 145:4880–4889. [PubMed: 15271881]
13. Kelly LJ, et al. Peroxisome proliferator-activated receptors gamma and alpha mediate in vivo regulation of uncoupling protein (UCP-1, UCP-2, UCP-3) gene expression. Endocrinology. 1998; 139:4920–4927. [PubMed: 9832429]
14. Rempe D, et al. Synapsin I Cre transgene expression in male mice produces germline recombination in progeny. Genesis. 2006; 44:44–49. [PubMed: 16419044]
15. Lu M, et al. Inducible Nitric Oxide Synthase Deficiency in Myeloid Cells Does Not Prevent Diet-Induced Insulin Resistance. Molecular endocrinology (Baltimore, Md.
16. Steele R. Influences of glucose loading and of injected insulin on hepatic glucose output. Annals of the New York Academy of Sciences. 1959; 82:420–430. [PubMed: 13833973]
17. Bandyopadhyay GK, Yu JG, Ofrecio J, Olefsky JM. Increased malonyl-CoA levels in muscle from obese and type 2 diabetic subjects lead to decreased fatty acid oxidation and increased lipogenesis; thiazolidinedione treatment reverses these defects. Diabetes. 2006; 55:2277–2285. [PubMed: 16873691]

18. Gayen JR, Gu Y, O'Connor DT, Mahata SK. Global disturbances in autonomic function yield cardiovascular instability and hypertension in the chromogranin a null mouse. Endocrinology. 2009; 150:5027–5035. [PubMed: 19819970]

19. Lu M, et al. A new antidiabetic compound attenuates inflammation and insulin resistance in Zucker diabetic fatty rats. American journal of physiology. 298:E1036–1048. [PubMed: 20159859]

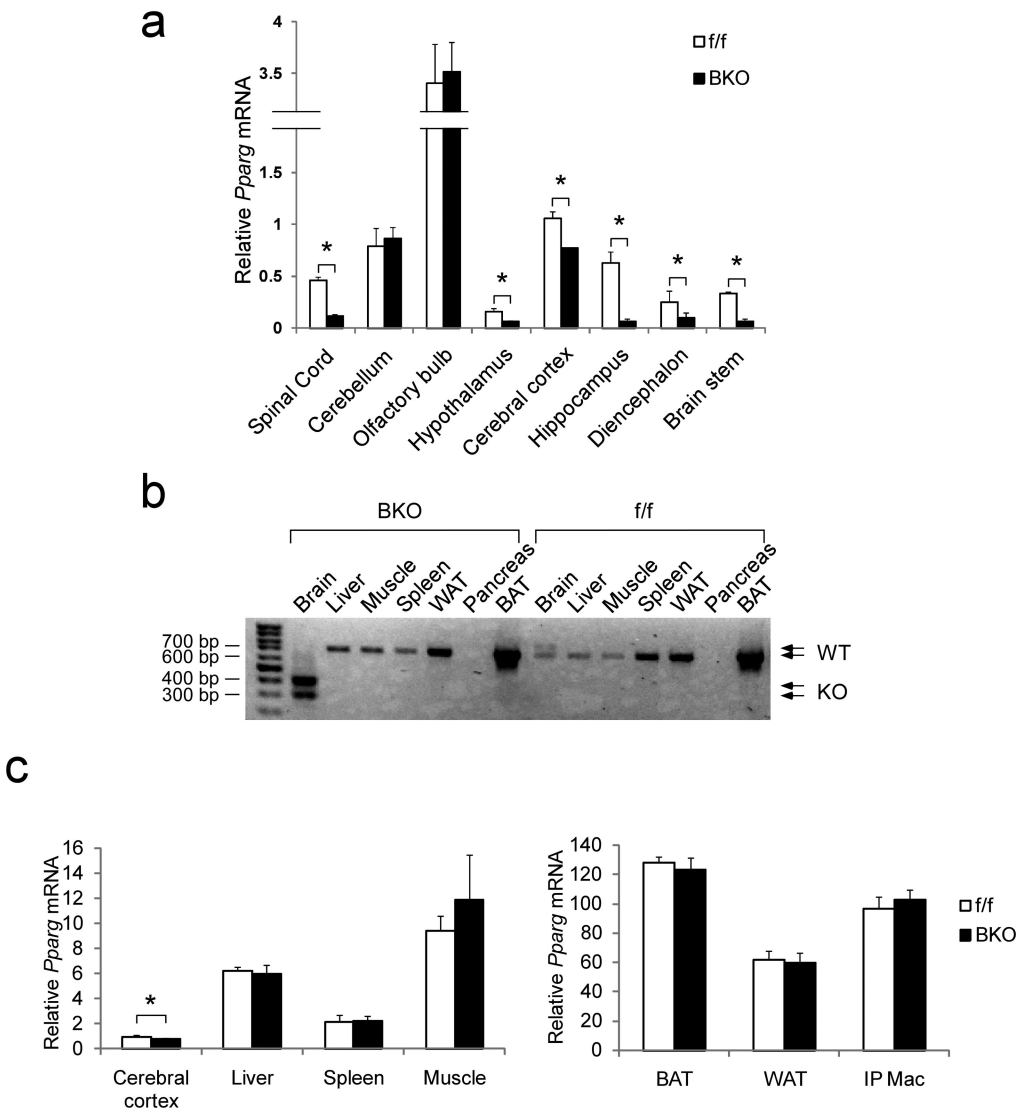

Fig. 1. Neuronal deletion of *Pparγ* in brain knockout mice

(**a**) Quantification of wild type *Pparγ* mRNA in various brain regions of *Pparγ* f/f mice and BKO mice. Data shown are the fold induction of gene expression normalized with housekeeping gene and expressed as mean ± SEM. (**b**) RT–PCR showing wild type and mutant (KO) *Pparγ* mRNA in various tissues in control and BKO mice. (**c**) Quantification of tissue *Pparγ* mRNA expression. Data shown are the fold induction of gene expression normalized with housekeeping gene and expressed as mean ± SEM. Asterisks indicate statistical significance ($p < 0.05$) between conditions connected by bars.

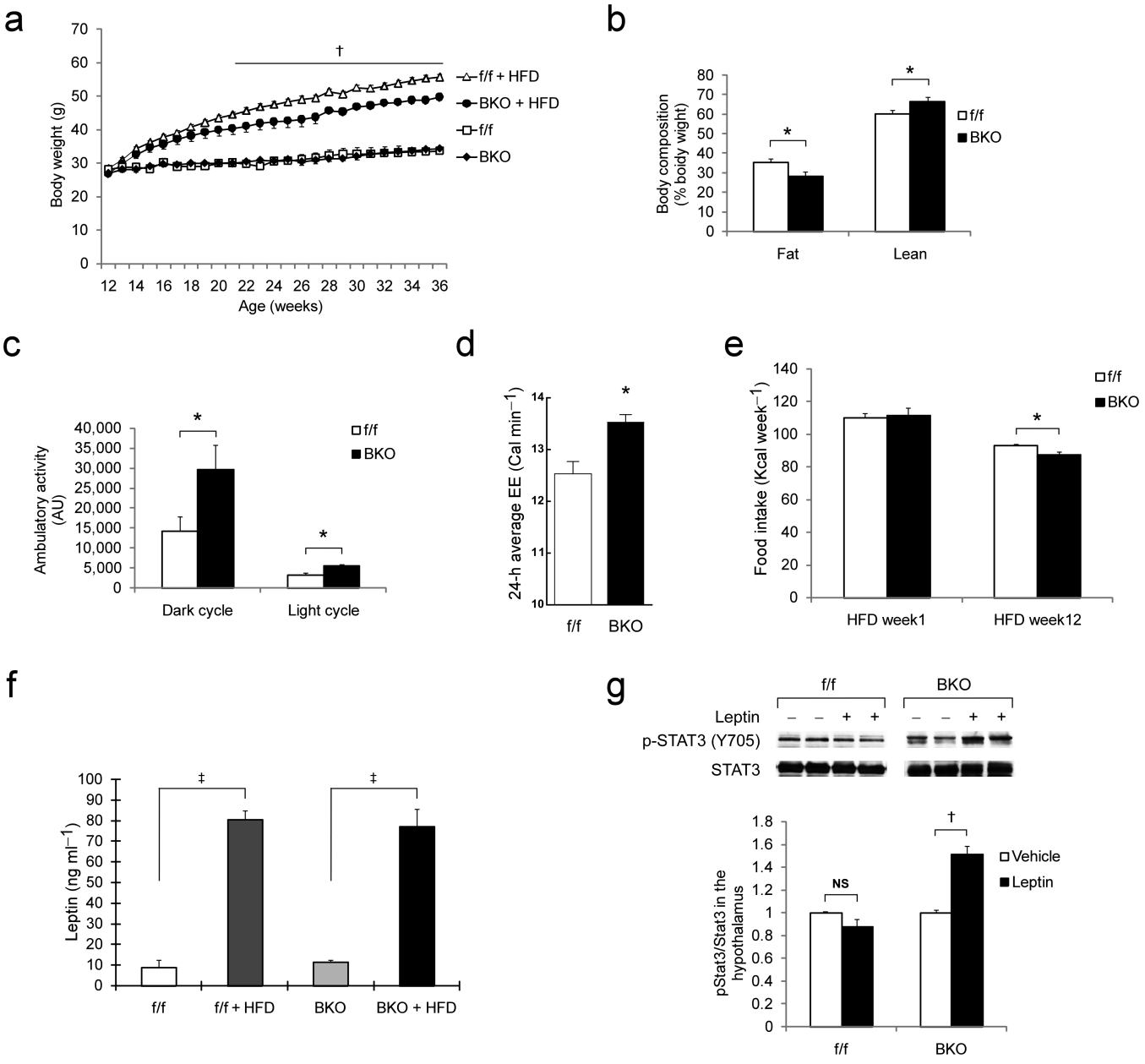

Fig. 2. Energy balance parameters in *Pparγ* brain KO mice

(**a**) Body weight of *Pparγ*–f/f and BKO mice on either standard chow or HFD. Dagger indicates statistical significance ($p < 0.01$) between genotypes. (**b**) Body composition analysis of control ($n = 8$) and *Pparγ* BKO ($n = 6$) mice at wk 5 on HFD. (**c**) Ambulatory activity of control ($n = 7$) and BKO ($n = 6$) mice at wk 6 on HFD. (**d**) Average 24–h energy expenditure in control ($n = 8$) and BKO ($n = 6$) mice after adjustment for body size differences and 24–h average activity. (**e**) Weekly caloric intake of control ($n = 12$) and BKO ($n = 11$) mice at weeks 1 and 12 on HFD. (**f**) Serum leptin concentration in control and BKO mice fed either standard chow or HFD ($n = 5$–9 per group). (**g**) Western blot showing acute leptin–stimulated phosphorylation of STAT3 (Y705) in hypothalamus. Data shown are quantified ratio of p–STAT3/total STAT3 normalized to vehicle group. All data are mean ±

SEM. Statistical significance between control and *Pparγ* BKO mice, or between conditions connected by bars, is indicated by asterisks ($p < 0.05$), daggers ($p < 0.01$), double daggers ($p < 0.001$), or NS (not significant).

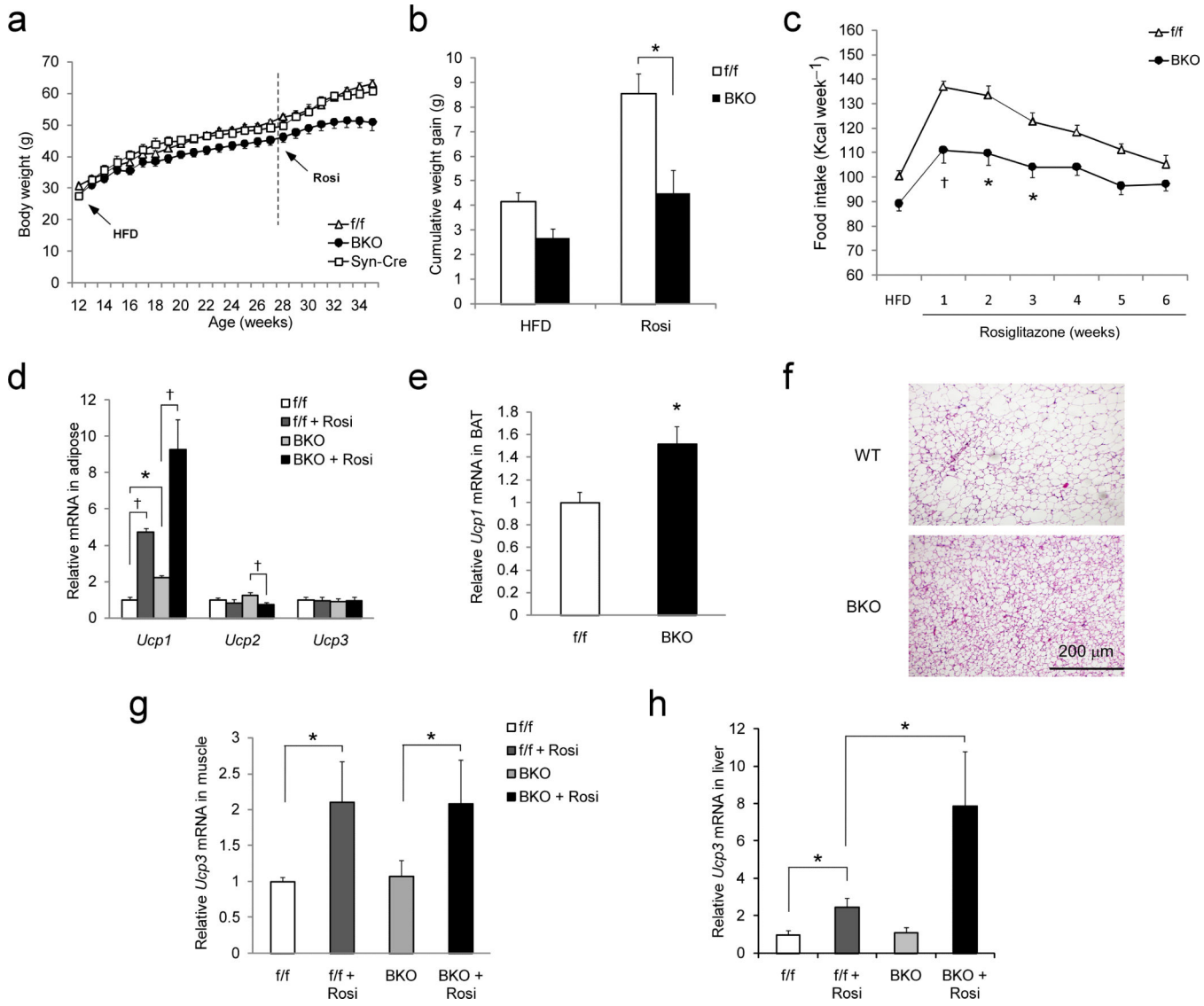

Fig. 3. Effect of rosiglitazone on weight gain and food intake in control and *Pparγ* BKO mice

(**a**) Rosiglitazone–induced weight gain in *Pparγ*f/f (*n* = 14), Syn–Cre (*n* = 6), and *Pparγ* BKO (*n* = 11) mice. Age of mice, start time of HFD, and HFD + rosiglitazone (rosi) are indicated. (**b**) Body weight gain of control and *Pparγ* BKO mice that were fed HFD for 16 wk followed by HFD with or without rosiglitazone treatment. Data are shown for weeks 28–34 (*n* = 6–14 per group). (**c**) Weekly caloric intake before and after rosiglitazone treatment in HFD-fed mice showing the effect of rosiglitazone on food intake in control (*n* = 14) and *Pparγ* BKO (*n* = 11) mice. (**d**) Measurement of *Ucp1* mRNA in epididymal white adipose tissue from control and *Pparγ* BKO mice. (**e**) BAT *Ucp1* mRNA expression in control and *Pparγ* BKO mice after rosiglitazone treatment. (**f**) Histochemical image of BAT from control and *Pparγ* BKO mice after rosiglitazone treatment stained with H&E. (**g**) Muscle *Ucp3* mRNA expression in control and *Pparγ* BKO mice on HFD with or without rosiglitazone treatment (*n* = 5–10 per group). (**h**) Liver *Ucp3* mRNA expression in control and *Pparγ* BKO mice on HFD or after rosiglitazone treatment (*n* = 5–10 per group). (**a**)–(**c**),

data are shown as mean ± SEM. (**d**)–(**h**), all qPCR data shown are the fold induction of gene expression normalized with housekeeping gene and expressed as mean ± SEM. Statistical significance between control and *Pparγ* BKO mice, or between conditions connected by bars, is indicated by asterisks ($p < 0.05$), daggers ($p < 0.01$), or NS (not significant).

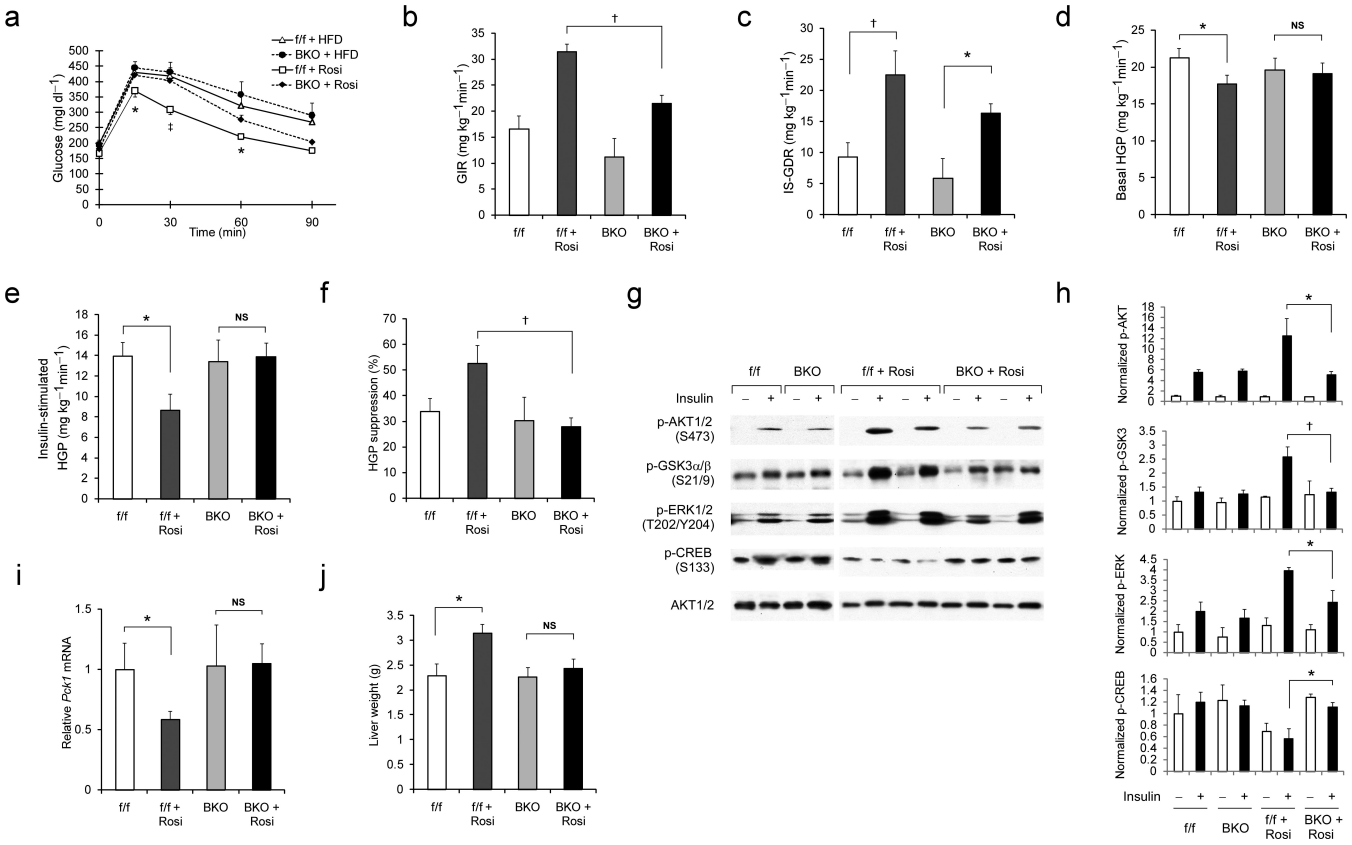

Fig. 4. Neuronal PPARγ is required for the full insulin–sensitizing effect of TZD treatment

(**a**) Intraperitoneal glucose tolerance tests (IPGTTs) on *Pparγ*f/f and BKO mice on HFD with or without rosiglitazone treatment for 7 wk (n = 6–12 per group). Statistical significance between values from rosiglitazone–treated control and *Pparγ* BKO mice indicated by asterisks ($p < 0.05$) and dagger ($p < 0.01$). (**b**)–(**f**), Hyperinsulinemic euglycemic clamp study on control and *Pparγ* BKO mice fed a HFD with or without rosiglitazone treatment for 8 wk (n = 7–12 per group). Glucose infusion rate (GIR) (**b**), insulin–stimulated glucose disposal rate (IS–GDR) (**c**), basal hepatic glucose production rate (basal HGP) (**d**), insulin–stimulated rate of HGP (**e**), and percent suppression of HGP by insulin (**f**) are shown. (**g**) Immunoblotting analysis of insulin-stimulated protein phosphorylation in liver extracts from control and BKO mice fed a HFD in the presence or absence of rosiglitazone treatment. (**h**) Quantification of relative phospho–protein levels normalized to respective total kinase protein content or β–tubulin. Data are shown as mean ± SEM. (**i**) Liver *Pck1* (*Pepck*) mRNA expression in control and BKO mice fed a HFD or after rosiglitazone treatment (n = 5–10 per group). (**j**) Liver weight of control and *Pparγ* BKO mice (n = 10–14 per group) on HFD with or without rosiglitazone treatment. All data shown are as mean ± SEM. Statistical significance between conditions connected by bars is indicated by asterisks ($p < 0.05$), daggers ($p < 0.01$), or NS (no significance).